THE DISTRIBUTION AND DEPOSITIONAL HISTORY OF SEDIMENTARY DEPOSITS IN ARABIA TERRA. K. J. Zabrusky[1], J. C. Andrews-Hanna[2], and S. M. Wiseman[3], [1]Department of Geology, Colorado School of Mines, Golden, CO, kzabrusk@mymail.mines.edu, [2]Department of Geophysics, Colorado School of Mines, Golden, CO, jcahanna@mines.edu, [3]Department of Geological Sciences, Brown University, Providence, RI

Introduction: Layered sedimentary deposits have been widely recognized in Sinus Meridiani, Meridiani Planum, and throughout Arabia Terra [1, 2]. In the type locality of Meridiani, these rocks are rich in sulfate minerals [3, 4], and exhibit unique erosional morphologies including pedestal craters, inverted craters, etched terrain, and buttes or knobs (Fig. 1). CRISM sulfate detections [5] and similar erosional patterns are seen in many other sedimentary rock outcrops throughout Arabia Terra. The similarity of these outlying deposits to Meridiani, and the eroded nature of both, suggests a common origin and that the deposits were once much more extensive [6, 7, 8]. Here, we present additional evidence for the relationship of these deposits from morphological observations. We then use crater age dating techniques to estimate the mean deposit age and to constrain the deposition and erosion rates.

Geomorphic Analysis: The sedimentary rocks within Meridiani erode into several unique morphologies. The etched terrain is noted for its highly textured pattern, caused by differential erosion of the layering (Fig. 1a). A similar erosional pattern is seen in the sedimentary infill of a crater located elsewhere in Arabia Terra (Fig. 1b). Pedestal craters occur in the layered rocks at the edge of Meridiani Planum (Fig. 1c); they are formed when sedimentary material under the ejecta of the crater is protected from erosion. The abundance of pedestal craters in Arabia Terra is here interpreted as marking the former extent of layered sedimentary deposits related to those in Meridiani. Figure 1d shows a portion of a degraded basin in northeast Arabia Terra (centered ~17.4ºN 20.5ºE) that was likely filled with sediments, the remnants of which are preserved in multiple pedestal craters (Fig. 2). Similarly, inverted sediment-filled craters also occur in both the layered sedimentary rocks of Meridiani (Fig. 1e), as well as in the aforementioned basin and elsewhere in Arabia Terra (Fig. 1f). Finally, buttes or knobs are common as eroded remnants in the layered sedimentary rocks of Meridiani (Fig. 1g). Similar structures are seen in the central mound of Pasteur Crater (Fig. 1h), suggesting an eroded remnant of a similar deposit.

Crater Counting: Size-frequency distributions of craters are commonly used to estimate the exposure age of a surface. The abundance of pedestal craters within the eroded remnants of the Arabia Terra deposits affords the unique opportunity to reconstruct the depositional and erosional history of these deposits. The degraded basin referred to earlier has a high density of pedestal craters, as well as craters both older and younger than the eroded deposit, making it a good candidate on which to perform crater age dating.

The JMARS software was used to catalog all craters larger than 1 km within the basin. Each crater was assigned an age in relation to the deposits of pre-, syn-, or post-deposit based on geomorphic criteria. Pre-deposit craters are visibly filled with layered deposits or are extremely degraded. Pedestal craters were classified as syn-deposit, as were craters that both occur on and are filled with layered deposits. It is not possible to distinguish between pedestal craters that formed during the deposition of the deposits and those that formed during their subsequent erosion. Thus, the syn-deposit crater population records both the deposition and erosion of the deposits. Post-deposit craters have ejecta that overlies the deposits, or have fresh morphologies (sharp rims and pristine ejecta blankets).

We then used the Craterstats software to assign ages to the stages of deposit formation and erosion. The crater retention age from the post-deposit craters

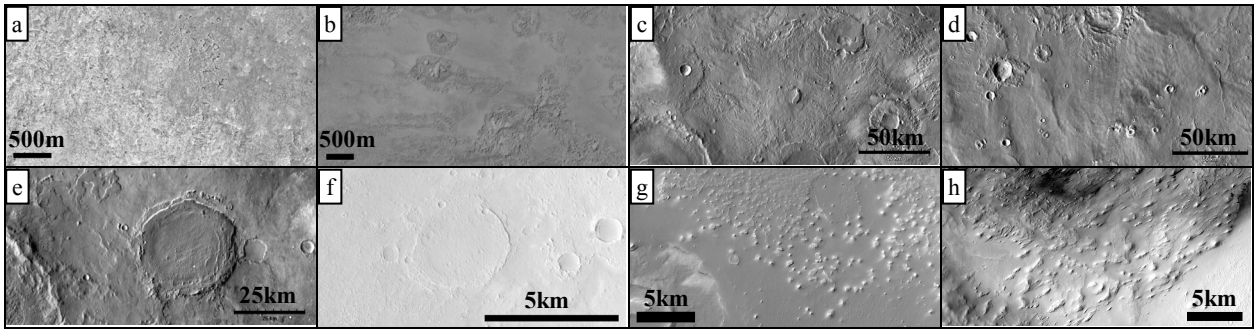

Figure 1. Morphologies unique to Meridiani-type deposits. See text for further descriptions. a: HiRISE ESP_016881_1805, b: P17_007571_1859_XI_05N335W, c: THEMIS 100m day IR, d: THEMIS 100m day IR, e: THEMIS 100m day IR, f: P15_006925_1955_XN_15N337W, g: B01_009840_1885_XN_08N010W, h: P02_001756_1994_XI_19N335W. North is up in all images.

records the age at which large-scale erosion of the deposits had largely ceased. The crater retention age from the combined post- and syn-deposit crater populations represents a mean age of the deposits themselves. The crater retention age of the post-, syn-, and pre-deposit crater populations represents the age prior to deposition. This latter age may under-estimate the onset age of deposition, as it is unlikely that all craters formed during and after deposition are perfectly preserved.

The total age of the pre-, syn-, and post-deposit craters within the basin is $3.88^{+0.02}_{-0.03}$ Ga. The post- and syn-deposit craters give an age of $3.56^{+0.05}_{-0.08}$ Ga, and the post-deposit craters alone give an age of $3.42^{+0.09}_{-0.28}$Ga (Fig. 3). Craters for which the ages relative to the deposits were ambiguous were reclassified to estimate the errors for each age category of ~0.04-0.2 Ga.

The crater populations within this filled and exhumed basin indicate that the layered sediments were laid down and subsequently eroded during a ~460 million year period between ~3.88 and ~3.42 Ga. This coincides with the Late Noachian through the first half of the Late Hesperian epochs, with a mean deposit age of Early Hesperian. This agrees with prior estimates of the age of major sulfate deposition [9], but provides a more refined history for these deposits. Assuming that deposition and erosion of the deposits occurred over equal time spans, and a mean deposit height of ~1 km within the basin, the mean deposition and erosion rates equal 4.3×10^{-6} m/yr. A lower bound on either the deposition or erosion rate, assuming that either stage lasted the full 460 Myr, is 2.2×10^{-6} m/yr. These rates are in accordance with other estimates for erosion rates on early Mars [10]. The deposition rate has been calculated for the Becquerel Crater deposits from the correlation of the layer periodicities with the orbital evolution of Mars [11], leading to rates of ~$3\text{x}10^{-5}$ m/yr. While our lower-bound on the deposition rate cannot rule out this higher rate, we note that hydrological models predict the rate of groundwater upwelling and sedimentation within Becquerel to be ~3× higher than the rate within this buried basin [7], bringing the calculated mean depositional rate within the basin into agreement with the scaled rate from Becquerel.

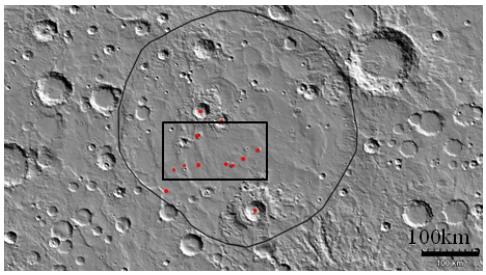

Figure 2. Regional view of basin (black outline) in MOLA topography. Red dots indicate pedestal craters. Box shows approximate location of Figure 1d. Basin is ~131,945 km^2.

Discussion and Conclusions: Geomorphic evidence suggests that outlying deposits throughout Arabia Terra are genetically related to those in Meridiani. Coupled with earlier work [7, 8], this study helps build the case that the outlying layered sedimentary rocks of Arabia Terra share a common origin with those in Meridiani, and that these deposits were once much more widespread prior to their erosion. We also used a basin in northeast Arabia Terra that was likely filled with the Meridiani-type deposits to estimate the formation and erosion history of the deposits. We found that the deposits were laid down between ~3.88 and ~3.42 Ga, with a lower bound on both the deposition and erosion rates of 2.2×10^{-6} m/yr. Significantly, the high erosion rates signal an epoch in which hydrological activity was waning or had ceased entirely, allowing the water table to drop below the surface to expose the deposits to aeolian deflation. Erosion rates at this time were comparable to those in arid regions of the Earth today [10], which may suggest a thick atmosphere was present even as Mars dried out in the Hesperian.

References: [1] Malin, M. C. and Edgett, K. S. (2000) *Science*, 290, pp. 1927-1937. [2] Hynek, B. M. and Phillips, R. J. (2008) *E&PSL*, 274, pp. 214-220. [3] Gendrin, A., et al. (2005) *Science*, 307, pp. 1587-1591. [4] Wiseman, S. M., et al. (2007) *7th Int'l Conf. on Mars,* Abstract #3111. [5] Wiseman, S. M. (2011) *LPS XLII*, this conference. [6] Hynek, B. M. (2004) *Nature*, 431, pp. 156-159. [7] Andrews-Hanna, J. C., et al. (2010) *JGR*, 115, p. 06002. [8] Zabrusky, K. J. and Andrews-Hanna, J. C. (2010) *LPS* XLI, Abstract #2529. [9] Carr, M. H. and Head, J. W. (2010) *E&PSL*, 294, pp. 185-203. [10] Golombek, M. P., et al. (2006) *JGR*, 111, E12. [11] Lewis, K. W., et al. (2008) *Science*, 322, p. 1532.

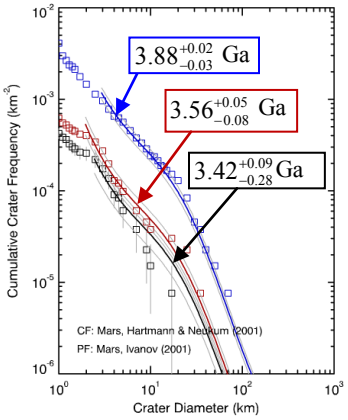

Figure 3. Crater size-frequency distributions showing post-deposition craters (black), post-deposition and syn-deposition craters (red) and all craters (blue). Error bars are light grey. CF= chronology function, PF= production function.